Barrier diffusion and optical properties of the Au-Al_2O_3-Al thin-film system

C. C. Chang and T. A. Callcott
Department of Physics and Astronomy, The University of Tennessee, Knoxville, Tennessee 37996
and Oak Ridge National Laboratory, Oak Ridge, Tennessee 37831

E. T. Arakawa
Oak Ridge National Laboratory, Oak Ridge, Tennessee 37831
(Received 20 September 1984)

The diffusion across the oxide barrier in a Au-Al_2O_3Al thin-film sandwich at temperatures below 300 °C has been studied in real time with use of an angular-reflectance method. Assuming a uniformly mixed alloy, the Maxwell Garnett equation was used to calculate the concentrations in the Al-diffused—in—Au layer from the reflectance data. The Al_2O_3 layer between the Au and Al films was formed by oxidation of Al in air. The rate of diffusion through the oxide did not have the usual inverse dependence on barrier thickness, but rather decreased exponentially with the oxide thickness and thus resembled the Al oxidation process. The data are consistent with a model in which Al ions migrate through the oxide under the influence of a strong electric field (about 5×10^6 V/cm) caused by the difference in the Fermi levels of Au and Al. The change of the work function of the Au-Al alloy for increasing Al concentration in Au is also calculated from the data.

I. INTRODUCTION

Diffusion in thin-film couples of Au and Al has been studied by several authors using optical methods. Weaver and Brown found that the normal incidence reflectance at the Au surface declined as the diffusion proceeded.[1] Loisel and Arakawa obtained more detailed results by observing the shift, during diffusion, of the angular position of the sharp minimum in the reflectance produced by surface plasmon resonance absorption.[2] In this study we have measured diffusion across a thin Al_2O_3 layer interposed between Au and Al, using an optical method involving measurements of the reflectance over a wide range of incident angles.

In the sandwich system, with a barrier of Al_2O_3, we find that Al is the mobile species and that diffusion proceeds more slowly than in a regular Au-Al diffusion couple at the same temperature. Moreover, we find no evidence in the data for the existence of well-defined plane boundaries separating different phases of the Au-Al alloy at 260 °C. On the contrary, the results are consistent with a model in which, at any instant, Al is dispersed uniformly throughout the Au layer as diffusion proceeds. This model is assumed in the following data analysis. Its justification is discussed further at the end of the paper.

It has been known for many years that the oxidation of Al in air proceeds very rapidly at the beginning, then slows down and almost stops.[3,4] For Al exposed to air, the oxide layer grows to be thicker than 10 Å in less than a half hour, but does not exceed 40 Å in one week.

Several types of evidence indicate that naturally grown Al_2O_3 films are uniform and free of pinholes. The natural oxide provides effective protection for clean aluminum. In the diffusion data, no back diffusion of Au into Al is observed as would be expected with interdiffusion through holes in the oxide. Electron microscopy studies performed at Oak Ridge National Laboratory on similarly prepared films with a resolution of 30 Å show no detectable holes for film thicknesses greater than 20 Å. Perhaps most convincingly, Al-Al_2O_3-Au structures make good tunneling junctions for oxide thicknesses exceeding 20 Å if care is taken to mask the metal layers so that they do not short together along the sample edges.

The oxidation process has been explained by N. F. Mott as follows.[5,6] Electron tunneling from Al to surface oxygen states establishes an electric field across the oxide; this field drives Al ions across the oxide and delivers them to the surface to form Al_2O_3. In this study, after the formation of an Al_2O_3 layer on the Al surface, we replace the adsorbed oxygen by evaporating a Au layer on the oxide. We interpret our data by assuming that the electric field generated by the work-function difference between Au and Al drives Al ions across the oxide to the Au layer in a manner similar to that of the oxidation process.

II. EXPERIMENTAL PROCEDURES

In this study, sample evaporation, annealing, and optical observations were performed in a vacuum chamber at a pressure of 5×10^{-6} Torr. Samples were left in the same chamber for subsequent diffusion measurements without exposure to the atmosphere, except during the deliberate production of oxide layers. Samples were prepared with the geometry shown in Fig. 1. First 600 Å of Au was evaporated on the flat side of a quartz semicylinder two inches in diameter. Then 50 Å of Al was evaporated on top of the Au film. The diffusion pump valve was then closed and pure oxygen was admitted into the chamber and left in the chamber for a period of time to oxidize the Al. For some samples, the vacuum pump was closed and the sample was allowed to oxidize in the ambient vacuum. The time of exposure was recorded.

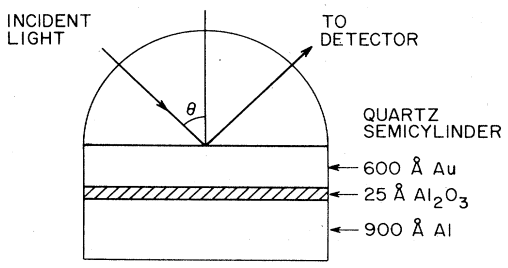

FIG. 1. Au-Al_2O_3-Al thin-film structure.

The chamber was pumped down again and the sample was raised to the selected diffusion temperature. When the diffusion temperature was reached, 900 Å of Al was evaporated on top of the oxide.

To heat the sample, two resistance heaters, one on top and the other at the bottom of the semicylinder, were turned on. Thermocouples were used to detect the temperatures at the top and at the bottom of the semicylinder. The electric currents flowing through the heaters were adjusted such that the temperature readings at the top and at the bottom of the semicylinder were the same. Because of the low thermal conductivity of quartz and the heat lost by radiation, the temperature rise at the center of the sample relative to room temperature was roughly 80% of the temperature rise detected at the top and the bottom of the semicylinder.

The reflectance as a function of incidence angle was measured repeatedly as diffusion proceeded. For these measurements, 5900-Å p-polarized light was incident through the curved surface of the semicylinder onto the Au surface of the sample as shown in Fig. 1. As the sample was rotated, light reflected from the quartz-Au interface was detected by a photomultiplier that rotated twice as fast as the sample to trace the reflected beam. The reflectance versus incident angle data at various times after deposition of Al were recorded and analyzed to get the diffusion depth.

The real part of the optical constant of Au has a large negative value for 5900-Å wavelength light so that the reflectance from the quartz-Au interface is very high. When an impurity is added to the Au layer or the Au layer becomes thinner in the diffusion process, the reflectance changes sensitively. Therefore, we chose 5900-Å light for our observations. We also used p-polarized light to simplify the calculation.

The Au layer of thickness 600 Å is thin enough to exhibit changes in reflectance when Al is diffused into it, yet is thicker than the light penetration depth. We will show later in this study that only the first layer is involved with the reflectivity, and calculations with simple optical equations are possible.

III. RESULTS AND DISCUSSION

A. Reflectance and diffusion depth

We had no independent means of determining the oxide barrier thickness, though estimates are possible from a knowledge of oxidation pressures and times. Oxide thickness information can, in principle, be obtained in several ways, including vuv optical measurements, visible wavelength ellipsometry, and electron tunneling, but none of these measurements could be readily carried out in our present apparatus. We hope to incorporate one or more of these measurements in future experiments made with redesigned equipment. For an oxide layer made by exposing Al to the air or to 1 atm. pressure of oxygen for one hour or more, the oxide layer approaches the saturation value of $\lesssim 40$ Å. The reflectances we observed on the thin-film systems for such thick oxide layers stayed stable for very long periods of time for diffusion temperatures below 300 °C, indicating that the diffusion rates were very low. For oxide layers prepared by exposing Al to less than 0.06 atm. of oxygen for less than 15 minutes, we obtained oxide layers of thicknesses between 10 and 30 Å which gave high diffusion rates at temperatures below 300 °C.

The diffusion phenomena can be compared to those of oxidation. For exposure times greater than one hour, the oxidation rate is slow. This corresponds to the slow diffusion region in our experiment. On the other hand, the oxidation rate is fast for oxidation times less than one-half hour, and this corresponds to our fast-diffusion region.

Data from a typical sample (sample 1) diffused at 260 °C are described below. The change of the angular reflectance $R(\theta)$ as diffusion proceeds is shown in Fig. 2. At all angles the reflectances decrease as diffusion proceeds. From the $R(\theta)$ values at six angles, using Fresnel's equations, the dielectric constants are calculated and shown in Fig. 3 as dots. In this sample it took about 80 minutes for the Au layer to be converted into the Au_2Al phase. In comparison, for a regular Au-Al diffusion couple, it would take about 0.2 s for the same Au and Al thicknesses to form Au_2Al at the same temperature.[2]

During the diffusion process, in which pure Au is converted to Au_2Al between the oxide barrier and the quartz substrate, no change in reflectance was observed on the Al side. In contrast, the reflectance at the quartz-Au interface changed very rapidly with time. This observation clearly indicates that Al rather than Au is diffusing through the oxide layer.

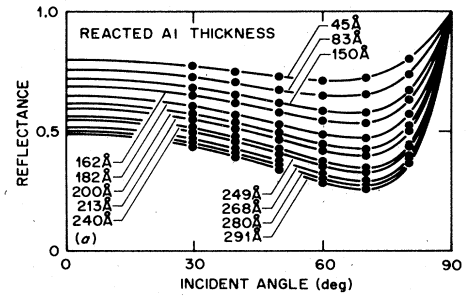

FIG. 2. Measured reflectances (dots) and the best fitting reflectances (solid curves) calculated using the dielectric constants along the solid curve of Fig. 3. The reacted Al thicknesses are indicated on the curves.

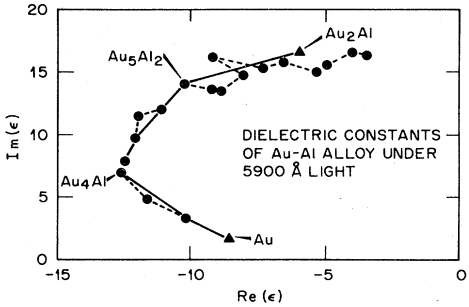

FIG. 3. Development with time of the observed dielectric constants (dots) and the dielectric constants calculated from the dielectric constants of Au, Au_4Al, Au_5Al_2, and Au_2Al (solid curve). The dielectric constants of Au and Au_2Al (triangles) are taken from the literature (Refs. 10 and 11).

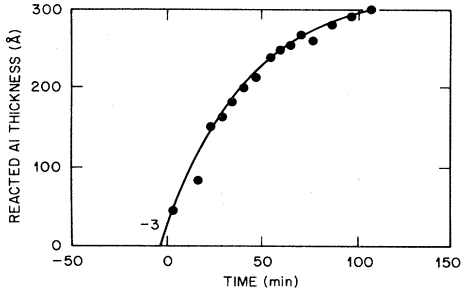

FIG. 4. Thickness of Al that has crossed the barrier and diffused into the Au layer as a function of time. The reacted Al thicknesses are from Fig. 2.

In the Au-Al_2O_3-Al sandwich structure, the diffusion of Al through the oxide is the rate-limiting process and the diffusion of Al in Au occurs much more rapidly. For reasons described in detail later, the Al-in-Au alloy is assumed to be a homogeneous layer. The problem then is to characterize the change in the optical properties of the Au-Al alloy as the concentration of Al increases from 0% to 33.3%.

The phase diagram of the Au-Al alloy system shows pure phases of Au, Au_4Al, Au_5Al_2, and Au_2Al for Al concentrations less than that of Au.[7] The concentrations of Al for these pure phases are 0, 20, 28.6, and 33.3 at. %, respectively. According to the lever rule, a well-mixed alloy at an arbitrary concentration is composed of two adjacent pure phases for the lowest Gibb's energy. Starting from pure Au, with Al increasing, the Au phase decreases and the Au_4Al increases. When the Al concentration C_{Al} is greater than 20%, the Au phase disappears and the alloy is a mixture of Au_4Al and Au_5Al_2. When C_{Al} is between 28.6% and 33.3% the alloy is a mixture of Au_5Al_2 and Au_2Al.

For a well-mixed alloy, when two phases exist simultaneously, the alloy consists of a mixture of small grains with pure phases. According to Maxwell Garnett's effective-medium equation,[8] the dielectric constant ϵ of the mixture can be related to the dielectric constants of the components by the equation

$$\frac{\epsilon-\epsilon_h}{\epsilon+2\epsilon_h}=\sum_i f_i\frac{\epsilon_i-\epsilon_h}{\epsilon_i+2\epsilon_h}\ , \tag{1}$$

where ϵ_h and ϵ_i are the dielectric constants of the major constituent and the minor constituents, respectively, and f_i are the volume ratios of the minor constituents in the mixture. Here we have only one minor phase each time. When there is no significant major phase in the alloy, we can let[9]

$$\sum_i f_i\frac{\epsilon_i-\epsilon}{\epsilon_i+2\epsilon}=0\ . \tag{2}$$

If the real part of the resultant dielectric function $\mathrm{Re}(\epsilon)$ is plotted versus the imaginary part $\mathrm{Im}(\epsilon)$, the curve will be smooth for concentrations between two adjacent pure phases. However, the curve will in general have a break in its slope when the concentration crosses a pure phase with one of the phases having disappeared and a new phase appearing. These breaks in the slope of the $\mathrm{Re}(\epsilon)$ vs $\mathrm{Im}(\epsilon)$ plot proved useful in the analysis of our data.

From Fig. 3 there are inflection points at $\epsilon=(-12.6,6.8)$ and at $(-10.2,13.9)$. These points are assumed to correspond to pure Au_4Al and Au_5Al_2 phases. By using Maxwell Garnett's equation and the Au-Al reaction formula, the dielectric constants of the alloy are found to join the inflection points smoothly as shown by the solid curve in Fig. 3. The end points of this curve are the known dielectric constants of Au and Au_2Al as $\epsilon=(-8.57,1.62)$ and $(-5.98,16.4)$, respectively.[10–12]

The reflectances calculated using dielectric constants obtained from the solid curve of Fig. 3 were compared with the experimental reflectance. A least-squares fit of reflectances made using various dielectric constants along the solid curve of Fig. 3 (i.e., various concentrations) was used in the reflectance comparison. The best fitting reflectance curve and the reacted Al thickness associated with it at each diffusion stage are shown in Fig. 2 with the Al thickness indicated on the curve.

The final result is shown in Fig. 4, which shows X_{Al}, the amount of reacted Al, as a function of time. X_{Al} increases rapidly at first and then slows down. When the curve is extrapolated to time $t=0$, the intersection shows $X_{Al}=25$ Å. This is approximately the thickness of the Al left in the layer after the oxidation process. When the curve is extrapolated to $X_{Al}=0$, the time is about -3

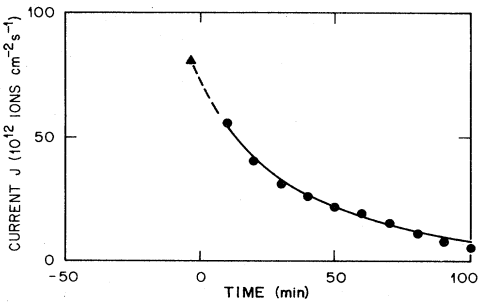

FIG. 5. Current density of Al atoms crossing the barrier as a function of time.

TABLE I. Experimental parameters for four barrier diffusion samples.

Sample	Oxidation conditions (Torr)	Oxidation time (min)	Diffusion temperature (°C)	Ion current at $C_{Al}=0$ (10^{12} cm^{-2}s^{-1})	Barrier thickness (Å)
1	40 (O_2)	5	260	80	28.5
2	760 (O_2)	10	244	2	39
3	5×10^{-6} (ambient vacuum)	10	90	150	13
4	5×10^{-4} (ambient vacuum)	6	137	10	17

min., which gives the effective start of time.

The diffusion flux J of Al atoms as a function of time may be calculated from the slope of Fig. 4. The plot of J versus time is shown in Fig. 5. The flux is seen to vary from $J=80\times10^{12}$ cm^{-2}s^{-1} at time -3 min to 5.5×10^{12} cm^{-2}s^{-1} at 100 min.

The results of several diffusion samples are summarized in Table I. The diffusion rate for sample 3 was very fast and was calculated from the time required for the Au layer to turn completely into Au_2Al. The diffusion rates for samples 2 and 4 were very slow, and were obtained from the changes in their optical constants for short time intervals in the initial stages of diffusion.

B. Diffusion mechanisms

In this study the diffusion rate for an Au-Al_2O_3-Al system is found to be controlled by diffusion through the oxide layer. The barrier diffusion does not obey the usual diffusion law. This can be seen as follows. At first, let us assume that the diffusion rate depends on the motion of particles in the oxide and does not depend on the rate of particles crossing the boundaries. When the diffusion in the oxide is in the steady state, according to Fick's law, the diffusion current J obeys the relation

$$J=-D\frac{\partial C}{\partial X}=-D\frac{\Delta C}{X}\ , \tag{3}$$

where D is the temperature-dependent diffusion coefficient, C is the concentration of Al, and X is the thickness of the oxide. Since the concentration difference is approximately 1 at the beginning and declines to 66.7% at the end of the experiment (Au_2Al phase), the flow of Al is inversely proportional to the thickness of the oxide X. For oxide thickness ranging between 10 and 40 Å for naturally grown Al oxides, the diffusion currents between different samples measured at the same temperature should not differ by a factor of more than 4.

We prepared several barrier diffusion samples at room temperature with a variety of oxide thicknesses ranging from 10—40 Å. The diffusion temperatures were fixed at about 230°C. The observed initial diffusion currents ranged from 2×10^{12} to 150×10^{12} cm^{-2}s^{-1}, indicating a factor of 75. The diffusion rate depends on the thickness of the oxide more strongly than that predicted by Fick's law in Eq. (3). In Fig. 5 the diffusion current J declined from 80×10^{12} cm^{-2}s^{-1} for $\Delta C_{Al}=-1$ to about 5.5×10^{12} cm^{-2}s^{-1} for $\Delta C_{Al}=-0.667$. This also cannot be explained by Eq. (3). Therefore, to explain our results, we employ Mott's electron tunneling and ion migration model.

In the formation of natural oxides, electron tunneling must accompany ion diffusion in order to maintain charge neutrality, and either process may be rate limiting under appropriate conditions. In our experiments, the Au and Al films were deliberately shorted together so that an external current could maintain the Fermi levels in alignment. Thus in our experiments only ion diffusion need be considered.

Figure 6 shows the electron potentials of Au, Al_2O_3, and Al. The aligned Fermi levels, combined with the different work functions of Al and Au, generate an electric field across the oxide equal to the work-function difference divided by the oxide thickness.

The diffusion of neutral metal atoms in insulators is usually very slow at low temperatures;[13] field-driven ion diffusion can produce much higher rates, however. Figure 7(a) illustrates the diffusion process. The barrier height for Al ions to jump into the oxide is U, and the barrier between positions in the oxide is W. An electric field reduces the barrier heights, as shown in Fig. 7(b). For a metal ion close to the insulator, the electric field decreases the activation energy for the ion to jump from the metal site to an interstitial site in the insulator.

The probability per unit time for an ion to jump from one potential minimum to the next in the direction of the applied field F is $\nu\exp(-W/kT)\exp(qaF/2kT)$, where ν is the ion vibration frequency, W the zero-field barrier height, q the ion charge, and a the distance between potential minima. The probability for a jump against

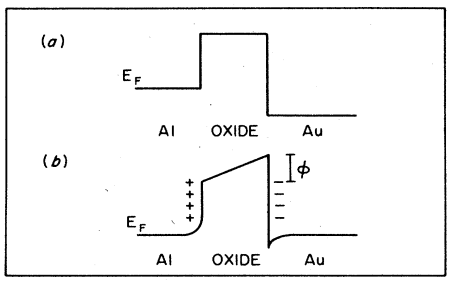

FIG. 6. (a) Electron potentials in the Au-Al_2O_3-Al structure before tunneling. (b) Electron potentials when the Al and Au layers are in electrical contact.

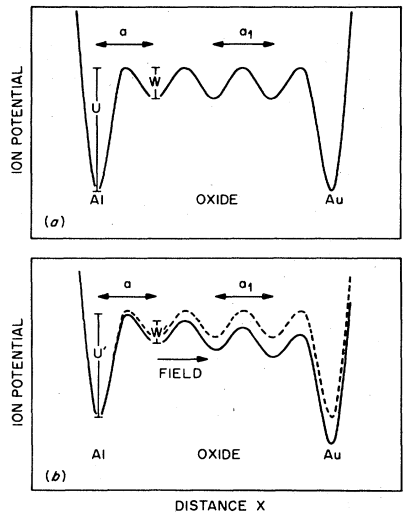

FIG. 7. (a) Ion potentials in the metal and in the oxide. (b) Ion potentials under an electric field.

the field is $\nu\exp(-W/kT)\exp(-qaF/2kT)$. For $qaF/2kT \gg 1$, as is the case here, the reverse current can be neglected.

We assume in our analysis the situation shown in Fig. 7(a), where the barrier (U) at the Al-Al_2O_3 interface is greater than the barriers within the oxide (W). In this case the rate-limiting process is the jump across the interface so that the ion current density may be written

$$J_{\text{ion}} = n\nu\exp(-U/kT)\exp(qaF/2kT) \tag{4}$$

and the electric current density is

$$I = qJ_{\text{ion}} . \tag{5}$$

Using the model parameters cited by Cabrera and Mott,[14] the ion charge is taken as $q=+3e$, $n=10^{15}/\text{cm}^2$ is the number of Al ions in the layer adjacent to the oxide, $\nu=10^{12}\ \text{s}^{-1}$, $U=1.8$ eV, and $a=7$ Å.

If ion migration within the oxide rather than ion injection through the metal-oxide interface is the rate-limiting process, the potential U in Eq. (4) should be replaced by the potential W and the exponential prefactor modified to account for multiple valleys. The foregoing analysis would not be significantly altered, however, by this alternative model, since the results are controlled primarily by the exponential factors.

Equation (4) indicates that J depends exponentially on the field strength F. F determined from J is plotted as a function of time for sample 1 in Fig. 8. When the curve of Fig. 8 is extrapolated to the time $t=-3$ min, where C_{Al} is defined to be zero, we have the initial field strength $F=3.83\times10^{-2}$ V/Å. F is equal to the potential drop divided by the oxide thickness. In the initial stages of diffusion, the potential drop is given by the difference in work function between Au and Al, i.e., $\phi=1.09$ V.[15] Using this value and the initial field strength for sample 1, the thickness of the oxide in this sample was found to be 28.5 Å. The oxide thicknesses of three other samples were

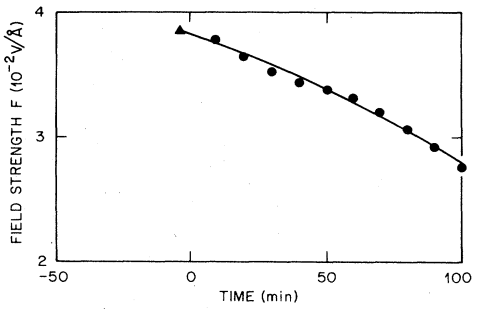

FIG. 8. Electric field strength within the oxide (dots). The triangle represents extrapolated value at $C_{\text{Al}}=0$.

determined in a similar fashion. The properties of these four samples are given in Table I. The calculated oxide thicknesses are consistent with values expected from other studies of the oxidation of Al, which show an initial rapid oxidation that saturates at a thickness of about 40 Å.[4]

When Al ions diffuse to the Au layer, more electrons will tunnel or flow through other paths to the Au layer to balance the ion charges and to reestablish the Fermi levels. The work function of Au decreases when Al is added to it as an impurity.[16] Thus the potential difference across the oxide decreases during the diffusion process and the diffusion current J decreases with time. There is evidence in the data that the work function of the Au layer is reduced by the addition of Al. Assuming a constant barrier thickness, the decrease of F with time visible in Fig. 8 is evidence for a change in the work function of the Au layer. The change in work function with Al concentration is shown in Fig. 9 for sample 1. The rise in Fermi level versus the impurity concentration curve showed an upward concavity. This is consistent with Friedel's model.[16]

Similar experiments have also been carried out with barrier layers of SiO and MgF_2. The qualitative results were similar to those reported above for Al_2O_3. However, it was not generally possible to get a uniform diffusion over a sufficiently large area to make reliable optical measurements. We believe that this is a result of the difficulty in evaporating sufficiently uniform insulating layers.

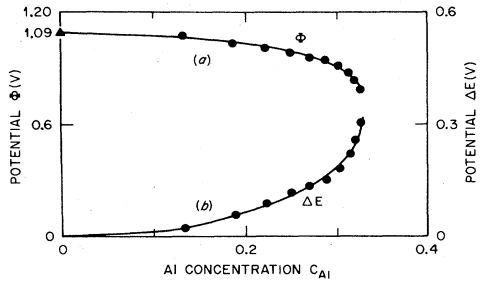

FIG. 9. (a) Potential difference (with left scale) across the oxide at different C_{Al}. (b) Calculated rise in the Fermi level (with right scale) of an Au layer with Al as the impurity.

C. Confirmation of the Au-Al alloy structure

We have seen above that reflectances are related to the diffusion. However, a model of the film structure is required in order to calculate the diffusion rate from the observed changes in reflectivity. The assumption that has been adopted above is that at 260 °C the Al-in-Au layer may be described at all concentrations as a single homogeneous layer. This implies that, at concentrations intermediate between pure phases, the layer is composed of a uniform mixture of small grains (less than the wavelength of light) of the two adjacent phases. Here we discuss an alternative model for this sample.

On the basis of regular diffusion in Au-Al couples,[17] we might have expected that each Al-richer phase would propagate with a plane boundary through the preceding Al-poorer phase. The model is illustrated in Fig. 10. As Al diffuses through the oxide layer into the two-phase Al-in-Au layer, the phase boundary propagates through the layer as shown by the arrows.

With the dielectric constants of the four pure phases the same as those mentioned before, the reflectance for light incident through the quartz substrate was calculated for this multilayer system for increasing Al concentrations. The results are shown as the dashed curve in Fig. 11 for reflectance at a 60° incidence angle where the reflectance change is sensitive to the change in Al concentration.

When such a multilayer model is applied to the barrier diffusion data we find that the calculated reflectance varies in a stair-step fashion because little change occurs in $R(\theta)$ until the new phase boundary moves close to the Au surface. However, the experimental reflectance is observed to change smoothly with time and to show no evidence of the stair-step changes in reflectance (Fig. 2).

We also show in Fig. 11 the reflectances at 60° for the experimental data and the values calculated with the uniform layer model (solid curve). Note that the multilayer model and the uniform layer model give the same result for single-phase alloys, but differ dramatically for concentrations that produce two-phase alloys. The essential feature of this comparison is that the experimental results show no trace of the stair-step variation of reflectance with time and with Al concentration that is predicted by the multilayer model.

In Fig. 2 we demonstrated good agreement between the angular reflectance data and reflectances calculated from the Maxwell Garnett equation. On the other hand, using the multilayer model and multilayer Fresnel's equation, the reflectance data do not fit any calculated curve except at the four pure phases.

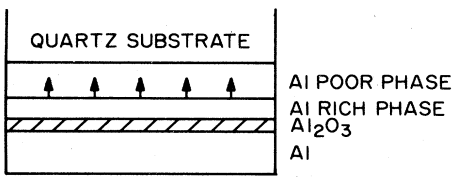

FIG. 10. Multilayer model for barrier diffusion experiment.

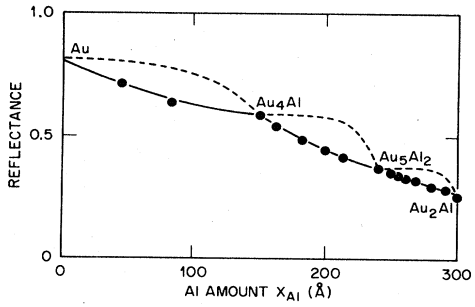

FIG. 11. Comparison of the reflectances at 60° at each reacted Al thickness for homogeneous model (solid curve) and layer model (dashed curve). Dots are data calculated using homogeneous model.

Clearly, our experimental results were in better agreement with the homogeneous layer model. This can be understood if at 260 °C the Gibb's energy for a crystallized atom is only slightly lower than that for a migrating atom along grain boundaries. In this case, atoms spend a significant fraction of their time as migrating atoms. With long migration times and high migration speeds, the migrating atoms can travel long distances. The high atom exchange rate prevents the Au-Al layer from forming an Al-richer region and an Al-poorer region. With the oxide acting as a barrier, the supply of Al to the alloy layer is not fast enough to support a sharp phase boundary in the alloy layer that would produce a fast net diffusion of Al. Therefore, the Au-Al alloy would be a well-mixed, two-phase layer rather than two layers separated by a moving phase boundary seen in regular diffusion.

IV. SUMMARY

Measurements of angular reflectance provide a convenient means of monitoring diffusion in thin-film systems nondestructively and in real time. The interpretation of reflectance data to obtain diffusion rates requires that some model be assumed for the structure of the system so that the reflectance can be calculated and related to the diffusion rates.

In this study of diffusion at temperatures between 90 and 260 °C across 10—40-Å Al_2O_3 barriers interposed between Al and Au layers, we were led by the data to a model of the diffusion process whose properties and consequences are summarized below.

(1) We find that Al, but not Au, diffuses through the barrier. In this diffusion process, penetration through the barrier and not diffusion in Au is the rate-limiting process.

(2) At 260 °C the observed reflectances were consistent with a model in which Al was dispersed uniformly throughout the Au layer in the form of finely mixed two-phase alloys, but were not consistent with a layered model in which successive phases were separated by plane boundaries.

(3) The observed dependences of the diffusion rates on

barrier thickness and temperature do not obey Fick's diffusion law for neutral atoms but are in good agreement with electric-field-driven diffusion of Al ions, where the driving field is produced by the work-function difference between the Al and Au layers. The process is similar to that operating in the oxidation of Al.

(4) Assuming field-driven diffusion, the data may be analyzed to determine oxide thicknesses. Oxide thicknesses ranging from 10—39 Å found in this way for our samples are consistent with those expected for natural oxides of Al. In addition, this model predicts that the decrease in diffusion rate with time is directly related to a decrease of the driving field and thus can be used to monitor the reduction in work function as Al is added to Au. We find a decrease in work function of Au of 0.3 V as the Al concentration increases from 0% to 33.3%.

ACKNOWLEDGMENTS

This paper represents a portion of a dissertation submitted by C. C. Chang to the University of Tennessee in partial fulfillment of the requirements for a Ph.D. degree. We want to thank J. E. Spruiell and F. Forstmann for valuable discussions. This research was sponsored by the Office of Health and Environmental Research, U. S. Department of Energy, under contract (Contract No. DE-AC05-84OR21400) with Martin Marietta Energy Systems, Inc.

[1]C. Weaver and L. C. Brown, Philos. Mag. **7**, 1 (1962).
[2]B. Loisel and E. T. Arakawa, Appl. Opt. **19**, 1959 (1980).
[3]R. P. Madden, L. R. Canfield, and G. Hass, J. Opt. Soc. Am. **53**, 620 (1963).
[4]G. Hass and M. H. Francombe, *Physics of Thin Solid Films* (Academic, New York, 1978), Vol. 10.
[5]N. F. Mott, Trans. Faraday Soc. **35**, 1175 (1939).
[6]N. F. Mott, Trans. Faraday Soc. **43**, 429 (1946).
[7]T. Lyman, *Metals Handbook* (American Society for Metals, Metals Park, Ohio, 1973), Vol. 8.
[8]J. C. Maxwell Garnett, Philos. Trans. R. Soc. London **203**, 385 (1904).
[9]D. A. G. Bruggeman, Ann. Phys. (N. Y.) **24**, 636 (1935).
[10]P. B. Johnson and R. W. Christy, Phys. Rev. B **6**, 4370 (1972).
[11]T. Inagaki, J. Appl. Phys. **52**, 5597 (1981).
[12]R. Stratton, J. Phys. Chem. Solids **23**, 1177 (1962).
[13]G. D. Bagratishvili, R. B. Dzhanelidze, D. A. Jishiashvili, L. V. Piskanovskii, and Z. N. Shiolashvili, Phys. Status Solidi A **56**, 27 (1979).
[14]N. Cabrera and N. F. Mott. Rep. Prog. Phys. **12**, 153 (1948).
[15]G. W. C. Kaye and T. H. Laby, *Tables of Physical and Chemical Constants* (Longman, New York, 1978).
[16]J. Friedel, Adv. Phys. **3**, 446 (1954).
[17]S. U. Campisano, G. Foti, E. Rimini, S. S. Lau, and J. W. Mayer, Philos. Mag. **31**, 903 (1975).